Vibrational Analysis of Ferrocyanide Complex Ion Based on Density Functional Force Field

Sun-Kyung Park, Choong-Keun Lee, Sang-Ho Lee,† and Nam-Soo Lee*

Department of Chemistry, Chungbuk National University, Cheongju, Chungbuk 361-763, Korea
†Biophysics Research Division and Department of Physics, The University of Michigan, Ann Arbor, MI 48109, USA
Received July 5, 2001

Vibrational properties of ferrocyanide complex ion, $[Fe(CN)_6]^{4-}$, have been studied based on the force constants obtained from the density functional calculations at B3LYP/6-31G** level by means of the normal mode analysis using new bond angle and linear angle internal coordinates recently developed. Vibrations of ferrocyanide were manipulated by twenty-three symmetry force constants. The angled bending deformations of C-Fe-C, the linear bending deformations of Fe-C≡N and the stretching vibrations of Fe-C have been quantitatively assigned to the calculated frequencies. The force constants in the internal coordinates employed in the modified Urey-Bradley type potential were evaluated on the density functional force field applied, and better interaction force constants in the internal coordinates have been proposed. The valence force constants in the general quadratic valence force field were also given. The stretch-stretch interaction and stretch-bending interaction constants are not sensitive to the geometrical displacement in the valence force field.

Keywords : Ferrocyanide, Vibrational analysis, Normal mode.

Introduction

Vibrational studies of molecules, metal complex ions, and other chemical systems have been direct methods approaching to understand the interatomic forces. The nature of metal-carbon bond in the transition metal-cyanide complexes derives considerable interests including σ-bonding or π-bonding characters and the force constant itself. Octahedral hexacyano transition metal complexes have inherent difficulties in assigning the vibrations of metal-carbon stretching, carbon-metal-carbon angled bending deformations, and metal-carbon-nitrogen linear bending deformations. Because it is strongly dependent on the bond strengths or distances of metal-carbon and carbon-nitrogen, vibrations can vary up to the centered transition metal atom, its oxidation state, or surrounding counter-cations. Vibrations of these metal complexes had been extensively studied by vibrational spectroscopic methods and normal mode calculations using the valence force field or the Urey-Bradley force field.[1-12] Also, *ab initio* or other quantum mechanical treatments[13,14] for these transition metal complexes of carbonyls as well cyanides have been performed for the vibrational properties or the electronic energies.

Applications of density functional theory[15] (DFT) to chemical systems have received much attention recently because of a faster convergence in time than the traditional quantum mechanical correlation methods in part, and improvements in the prediction of the molecular properties, *i.e*., the force field, vibrational frequencies, and dipole moments. Therefore the force field from DFT calculation has been utilized with the spectroscopic measurements for the assignment of observed frequencies and the refinements of the molecular force field under study. The normal mode analysis using Wilson's *GF* matrix formulation has been applied to elucidate the molecular systems of chemistry and biological sciences.[16,17] This matrix method has been enforced with improvements in the setup of internal coordinates,[18] the transferable scaling factors for various functional groups,[19] or in the computational method for the refinement procedure of the force field. It is now in progress to expand its application areas to molecular dynamics studies as well as structural studies.

In the present study, the vibrational analysis of octahedral ferrocyanide complex ion, $[Fe(CN)_6]^{4-}$, was performed by normal mode analysis method using the density functional force constant matrices to clarify the vibrational structure. The stretching vibrations of Fe-C, the angled bending deformations of C-Fe-C, and the linear bending deformations of Fe-C≡N have been quantitatively assigned to the calculated frequencies. Also we attempted to understand what changes could be induced in the interaction force constants upon geometrical displacement, and to obtain the force constants in the internal coordinates of the general quadratic valence force field or the modified Urey-Bradley type potential function applied to the study of ferrocyanide.

Calculation Methods

Four different geometries of ferrocyanide complex ion, *i.e*., geometry **A**, **B**, **C** and **Opt** are shown in Table 1. The geometry **Opt** is a fully optimized structure. The geometry **A**, **B**, and **C** are a little distorted structures to take the effects on the force field caused from the geometrical displacement. The structural feature of ferrocyanide with charge -4 and spin multiplicity 1 was applied to the Gaussian package[20] for the calculation of force constants matrix and intensities of Raman and IR bands at a certain geometry using the 6-31G** basis set under the B3LYP functional level. Calculat-

Table 1. Structural parameters, Electronic energies (ΔE_{elec}/kcal/mol) and Summations (ΔG_T/kcal/mol) of electronic and thermal free energies of three different geometries **A**, **B**, and **C** relative to **Opt**, and Optimized structural parameters of Ferrocyanide complex ion at various levels of theory

	Structural Parameters and Energies Calculated at B3LYP/6-31G**				Optimized Structural Parameters of $[Fe(CN)_6]^{4-}$				
	Geometry				B3LYP	B3LYP	HF	MP2	MP2
	A	**B**	**C**	**Opt**[a]	6-31+G**	6-31G (3df, 3pd)	6-31G**	6-31G**	6-31+G**
Fe-C	1.900 Å	1.910 Å	1.910 Å	2.009 Å	2.018 Å	2.010 Å	2.325 Å	1.860 Å	1.844 Å
C≡N	1.184 Å	1.184 Å	1.190 Å	1.184 Å	1.187 Å	1.176 Å	1.158 Å	1.204 Å	1.209 Å
ΔE_{elec}	8.0	6.4	6.6	0.0					
ΔG_T	10.0	8.3	9.3	0.0					

[a] fully optimized geometry

ed Cartesian force constants were transformed to a set of force constants in the symmetry coordinates or in the internal coordinates. Normal mode frequencies of vibrations were calculated using the Wilson's *GF* matrix method.

The chemical structure of ferrocyanide complex ion is shown in Figure 1 with an index number for each atom. The isotope atomic masses applied were 12.01115 for carbon, 14.00307 for nitrogen, and 55.84700 for Iron(II), respectively. The internal coordinates of ferrocyanide with total 13 atoms consist of twelve stretching internal coordinates (Δr) numbered R1 to R12, and twenty four deformation internal coordinates ($\Delta\theta$) numbered R13 to R36. Half of the deformations are the bond-angle deformations numbered R13 to R24, and the rest are linear angle deformations numbered R24 to R36. They are defined based on the atomic numbering scheme in Figure 1. New internal coordinate system[18] for the bond-angle deformation was adapted. As an internal coordinate of the bond-angle deformation, the half distance between two end points of two bonds connected was employed as given in Table 2. For a linear angle deformation, two torsion angles, θ_u (= 0°) and θ_w (= 90°), were introduced as internal coordinates as shown in Table 2 because each

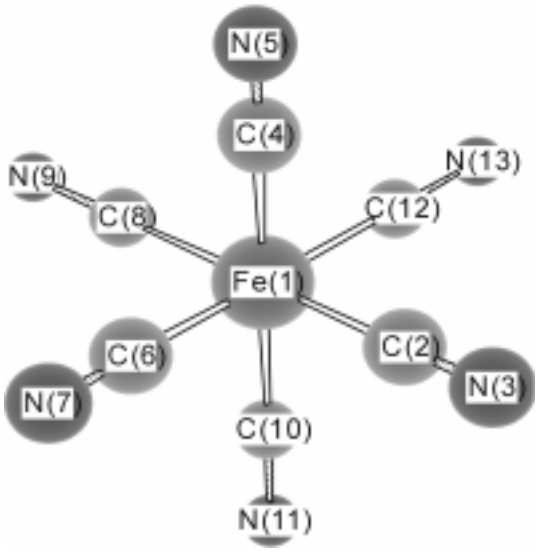

Figure 1. Chemical structure of ferrocyanide complex ion with the indexing numbers.

Table 2. Internal Coordinates of Ferrocyanide Complex Ion (R: the index number of internal coordinates, Atoms: Connections indicated with the index number shown in Figure 1.) and Molecular Structural Parameters applied for Geometry **B**

R	Name[a]	Atoms	Geometry	Parameters
R1	Δr(Fe-C)	1-2	1.910 Å	1.910 Å
R2	Δr(Fe-C)	1-4	1.910 Å	1.910 Å
R3	Δr(Fe-C)	1-6	1.910 Å	1.910 Å
R4	Δr(Fe-C)	1-8	1.910 Å	1.910 Å
R5	Δr(Fe-C)	1-10	1.910 Å	1.910 Å
R6	Δr(Fe-C)	1-12	1.910 Å	1.910 Å
R7	Δr(C≡N)	2-3	1.184 Å	1.184 Å
R8	Δr(C≡N)	4-5	1.184 Å	1.184 Å
R9	Δr(C≡N)	6-7	1.184 Å	1.184 Å
R10	Δr(C≡N)	8-9	1.184 Å	1.184 Å
R11	Δr(C≡N)	10-11	1.184 Å	1.184 Å
R12	Δr(C≡N)	12-13	1.184 Å	1.184 Å
R13	$\Delta\theta$(C-Fe-C)	2-1-4	90.0°	1.351
R14	$\Delta\theta$(C-Fe-C)	2-1-6	90.0°	1.351
R15	$\Delta\theta$(C-Fe-C)	4-1-6	90.0°	1.351
R16	$\Delta\theta$(C-Fe-C)	4-1-8	90.0°	1.351
R17	$\Delta\theta$(C-Fe-C)	6-1-8	90.0°	1.351
R18	$\Delta\theta$(C-Fe-C)	2-1-10	90.0°	1.351
R19	$\Delta\theta$(C-Fe-C)	6-1-10	90.0°	1.351
R20	$\Delta\theta$(C-Fe-C)	8-1-10	90.0°	1.351
R21	$\Delta\theta$(C-Fe-C)	2-1-12	90.0°	1.351
R22	$\Delta\theta$(C-Fe-C)	4-1-12	90.0°	1.351
R23	$\Delta\theta$(C-Fe-C)	8-1-12	90.0°	1.351
R24	$\Delta\theta$(C-Fe-C)	10-1-12	90.0°	1.351
R25	$\Delta\theta$(Fe-C≡N)	1-2-3	180.0°	0°
R26	$\Delta\theta$(Fe-C≡N)	1-2-3	180.0°	90°
R27	$\Delta\theta$(Fe-C≡N)	1-4-5	180.0°	0°
R28	$\Delta\theta$(Fe-C≡N)	1-4-5	180.0°	90°
R29	$\Delta\theta$(Fe-C≡N)	1-6-7	180.0°	0°
R30	$\Delta\theta$(Fe-C≡N)	1-6-7	180.0°	90°
R31	$\Delta\theta$(Fe-C≡N)	1-8-9	180.0°	0°
R32	$\Delta\theta$(Fe-C≡N)	1-8-9	180.0°	90°
R33	$\Delta\theta$(Fe-C≡N)	1-10-11	180.0°	0°
R34	$\Delta\theta$(Fe-C≡N)	1-10-11	180.0°	90°
R35	$\Delta\theta$(Fe-C≡N)	1-12-13	180.0°	0°
R36	$\Delta\theta$(Fe-C≡N)	1-12-13	180.0°	90°

[a]Δr: stretching of a bond length, $\Delta\theta$: bending of a bond angle.

Table 3. Symmetry Coordinates applied to Ferrocyanide Complex Ion (S: the index number of symmetry coordinates, R: the index number of internal coordinates listed in Table 2, Redundant coordinates of the angled bending deformations are not listed.)

S	Symbol[a]	Composition of Symmetry Coordinate	Descriptions
1	$\nu_{mc}(A_{1g})$	+R1+R2+R3+R4+R5+R6	Fe-C Stretching
2	$\nu_{mc}(E_g)$	+R2-R3+R5-R6	Fe-C Stretching
3	$\nu_{mc}(E_g)$	+2R1-R2-R3+2R4-R5-R6	Fe-C Stretching
4	$\nu_{mc}(T_{1u})$	+R1R4	Fe-C Stretching
5	$\nu_{mc}(T_{1u})$	+R2-R5	Fe-C Stretching
6	$\nu_{mc}(T_{1u})$	+R3-R6	Fe-C Stretching
7	$\nu_{cn}(A_{1g})$	+R7+R8+R9+R10+R11+R12	C≡N Stretching
8	$\nu_{cn}(E_g)$	+R8-R9+R11-R12	C≡N Stretching
9	$\nu_{cn}(E_g)$	+2R7-R8-R9+2R10-R11-R12	C≡N Stretching
10	$\nu_{cn}(T_{1u})$	+R7-R10	C≡N Stretching
11	$\nu_{cn}(T_{1u})$	+R8-R11	C≡N Stretching
12	$\nu_{cn}(T_{1u})$	+R9-R12	C≡N Stretching
13	$\delta_a(T_{2g})$	-R13+R16+R18-R20	Angled Bending
14	$\delta_a(T_{2g})$	-R14+R17+R21-R23	Angled Bending
15	$\delta_a(T_{2g})$	-R15+R19+R22-R24	Angled Bending
16	$\delta_a(T_{1u})$	-R13-R15-R16+R18+R19+R20-R22+R24	Angled Bending
17	$\delta_a(T_{1u})$	-R13-R14+R16+R17-R18+R20-R21+R23	Angled Bending
18	$\delta_a(T_{1u})$	-R14-R15-R17-R19+R21+R22+R23+R24	Angled Bending
19	$\delta_a(T_{2u})$	-R13+R15-R16+R18-R19+R20+R22-R24	Angled Bending
20	$\delta_a(T_{2u})$	-R13+R14+R16-R17-R18+R20+R21-R23	Angled Bending
21	$\delta_a(T_{2u})$	-R14+R15-R17+R19+R21-R22+R23-R24	Angled Bending
22	$\delta_l(T_{1g})$	+R25+R29-R31-R35	Linear Bending
23	$\delta_l(T_{1g})$	+R26+R28+R32+R34	Linear Bending
24	$\delta_l(T_{1g})$	-R27+R30+R33+R36	Linear Bending
25	$\delta_l(T_{2g})$	+R25-R29-R31+R35	Linear Bending
26	$\delta_l(T_{2g})$	+R26-R28+R32-R34	Linear Bending
27	$\delta_l(T_{2g})$	+R27+R30-R33+R36	Linear Bending
28	$\delta_l(T_{1u})$	+R25+R27+R31+R33	Linear Bending
29	$\delta_l(T_{1u})$	+R26+R30-R32-R36	Linear Bending
30	$\delta_l(T_{1u})$	-R28-R29+R34-R35	Linear Bending
31	$\delta_l(T_{2u})$	+R25-R27+R31-R33	Linear Bending
32	$\delta_l(T_{2u})$	+R26-R30-R32+R36	Linear Bending
33	$\delta_l(T_{2u})$	-R28+R29+R34+R35	Linear Bending

[a] ν_{mc}: Fe-C stretching mode, ν_{cn}: C≡N stretching mode, δ_a: angled bending mode, δ_l: linear bending mode.

linear angle deformation has degrees of freedom of two. They were defined from an arbitrary reference atom chosen nearby linearly aligned three atoms.

Symmetry coordinates adapted for ferrocyanide are displayed in the non-normalized format in Table 3 with descriptions for the nature of vibrations in terms of the internal coordinates R defined in Table 2. A complete set of thirty-three symmetry coordinates numbered 1 to 33 was constructed eliminating all the redundant symmetry coordinates occurred from angled bending deformations. There are six stretching modes (symbol name: ν_{mc}) for the Fe-C stretchings numbered 1 to 6, six stretching modes (symbol name: ν_{cn}) for the C≡N stretchings numbered 7 to 12, nine bond-angle deformation modes (symbol name: δ_a) for the angled C-Fe-C bending numbered 13 to 21, and twelve linear angle deformation modes (symbol name: δ_l) for the linear Fe-C≡N bending numbered 22 to 33.

The force constants matrix in the Cartesian coordinate generated through density functional calculation has 780 elements overall which are composed of all the diagonal and half the off-diagonal elements. When it is transformed to the symmetry coordinate, it becomes a matrix with 561 elements. These are too many to account for, so reduced to a comparable number of force constants using a boundary value in the symmetry coordinate. The force constants matrix of 561 elements could be extracted to 60 elements when the absolute values less than 0.004 of the off-diagonal matrix elements are eliminated and all the diagonal matrix elements are included. This boundary value 0.004 was rather arbitrary chosen because the off-diagonal elements less 0.004 are presumed to be minimal enough to be neglected for the structural elucidation. In fact, applying these 60 elements to calculation gives almost the same results in frequencies and potential energy distributions as 561 elements are applied. Because the ferrocyanide complex ion is highly symmetric belonging to a point group O_h, these 60 elements actually correspond to 23 elements in the symmetry species coordinate as shown in Table 4 for a fully optimized structure, the geometry **Opt**. The force constants for geometry **A**, **B**, and **C** are displayed in Table 5, which were transformed to the symmetry coordinate from Cartesian coordinate. The matrix of these force constants was then transformed back to a matrix in the Cartesian coordinate, then which was applied to calculate the frequencies using Wilson's *GF* matrix method. Using these values, the frequencies and potential energy distributions were obtained and given in Table 6 in terms of symmetry coordinates defined in Table 3.

The scaling factors are now well recognized to be transferable for the frequencies of organic functional groups. In this study, however, we did not apply any scaling factor, *e.g.*, 0.96, etc., for the frequency calculations even though the C≡N stretching frequencies are calculated a little higher. The vibrational frequencies of both stretching and deformations involving the centered metal atom are calculated well behaving to the experimentally observed ones. Partly because we believe that the vibrational data for vibrations involving the transition metal-carbon bonding have not been widely accumulated from the density functional force field we are currently utilizing. Table 1 also strongly suggests that the bond distances are quite dependent on the functional basis set that is to be selected for calculation.

Results and Discussion

Geometry and DFT Calculations. It has been experimentally known that the equilibrium distances in the ground low spin state $[Fe(CN)_6]^{4-}$ ion are positioned between 1.90

Table 4. Symmetry Force Constants (mdyn/Å, mdyn/rad, mdynÅ/(rad)^2) obtained from Density Functional Calculation for fully Optimized Geometry **Opt** (Fe-C: 2.009 Å, C≡N: 1.184 Å). (The bold faced symbol **S** represents the classification of vibrational modes for $M(CN)_6^{x-}$ type ionic species upon I. Nakagawa and T. Shimanouchi in Reference 1.)

		A_{1g}	E_g	T_{1u}	A_{1g}	E_g	T_{1u}	T_{2g}	T_{1u}	T_{2u}	T_{1g}	T_{2g}	T_{1u}	T_{2u}
		Fe-C Stretching			C≡N Stretching			C-Fe-C Angled Bending			Fe-C≡N Linear Bending			
		S_2	**S_4**	**S_7**	**S_1**	**S_3**	**S_6**	**S_{11}**	**S_9**	**S_{13}**	**S_5**	**S_{10}**	**S_8**	**S_{12}**
$\nu_{mc}(A_{1g})$	**S_2**	1.2599												
$\nu_{mc}(E_g)$	**S_4**		1.2126											
$\nu_{mc}(T_{1u})$	**S_7**			0.7796										
$\nu_{cn}(A_{1g})$	**S_1**	0.3053			17.4992									
$\nu_{cn}(E_g)$	**S_3**		0.2220			17.0028								
$\nu_{cn}(T_{1u})$	**S_6**			0.2134			17.0499							
$\delta_a(T_{2g})$	**S_{11}**							0.6010						
$\delta_a(T_{1u})$	**S_9**			-0.1154			0.1168		0.9292					
$\delta_a(T_{2u})$	**S_{13}**									0.7420				
$\delta_l(T_{1g})$	**S_5**										0.3196			
$\delta_l(T_{2g})$	**S_{10}**							-0.0282				0.4006		
$\delta_l(T_{1u})$	**S_8**			0.0418			0.0328		-0.1017				0.4311	
$\delta_l(T_{2u})$	**S_{12}**									-0.1340				0.4036

Table 5. Symmetry Force Constants (mdyn/Å or equivalents) from Density Functional Calculations for Geometry A, B, and C, and Refined Force Constants of Geometry B through Non-linear least-square fitting

Symmetry Species	S_i,S_j	Geometry **A** Fe-C: 1.90 Å C≡N: 1.184 Å	Geometry **B** Fe-C: 1.91 Å C≡N: 1.184 Å	Geometry **C** Fe-C: 1.91 Å C≡N: 1.190 Å	Refined Force Constants of Geometry **B**
A_{1g}	**S_1,S_1**	17.5531	17.5479	16.8620	16.840
	S_1,S_2	0.3575	0.3531	0.3506	0.725
	S_2,S_2	2.3709	2.2437	2.2397	2.424
E_g	**S_3,S_3**	16.9657	16.9700	16.2922	16.270
	S_3,S_4	0.3708	0.3563	0.3550	0.660
	S_4,S_4	2.3582	2.2298	2.2261	2.184
T_{1g}	**S_5,S_5**	0.3335	0.3329	0.3944	0.333
T_{1u}	**S_6,S_6**	16.9945	17.0000	16.3190	16.000
	S_6,S_7	0.3612	0.3465	0.3452	0.523
	S_6,S_8	0.0382	0.0371	0.0378	0.038
	S_6,S_9	0.1701	0.1645	0.1637	0.165
	S_7,S_7	1.6340	1.5371	1.5313	1.640
	S_7,S_8	0.0437	0.0435	0.0431	0.038
	S_7,S_9	- 0.1110	- 0.1117	- 0.1130	- 0.118
	S_8,S_8	0.4813	0.4765	0.6000	0.448
	S_8,S_9	- 0.1626	- 0.1568	- 0.0668	-0.129
	S_9,S_9	0.8296	0.8429	0.9070	0.835
T_{2g}	**S_{10},S_{10}**	0.4457	0.4416	0.5653	0.407
	S_{10},S_{11}	- 0.0727	- 0.0683	- 0.0042	-0.105
	S_{11},S_{11}	0.5822	0.5862	0.6166	0.553
T_{2u}	**S_{12},S_{12}**	0.4455	0.4417	0.5648	0.442
	S_{12},S_{13}	- 0.1881	- 0.1829	- 0.0938	-0.183
	S_{13},S_{13}	0.5723	0.5941	0.6561	0.594

and 1.98 Å for Fe-C and between 1.12 and 1.19 Å for C≡N depending on the positively charged counter-cations. Sano et al[21] chose the Fe-C bond distance as 1.925 Å and the C≡N as 1.167 Å to correlate the photoelectron spectrum of $K_4[Fe(CN)_6]$ to the molecular orbital calculation results. Mandix *et al.*[22] took the same bond distances as Sano *et al.*'s for the electron density distributions from *ab initio* HF calculation. Bolvin[23] chose the C≡N bond distance to a fixed 1.17 Å for the calculation of Fe-C distance with the complete active space (CAS) second-order perturbation function at a

Table 6. Observed and Calculated Vibrational Frequencies in cm^{-1} and Potential Energy Distributions for Geometry A, B, C and Opt using the Force Constants shown in Table 4 and 5

Vib. No.	Obs.[a]	Geometry **A**		Geometry **B**		Geometry **C**		Geometry **Opt**	
		Calc.	PED (greater than 5 %)	Calc.	PED (greater than 5 %)	Calc.	PED (greater than 5 %)	Calc.	PED (greater than 5 %)
ν_1	2098	2165.7	98 $\nu_{cn}(A_{1g})$	2163.4	98 $\nu_{cn}(A_{1g})$	2121.5	98 $\nu_{cn}(A_{1g})$	2145.7	100 $\nu_{cn}(A_{1g})$
ν_3	2062	2128.7	98 $\nu_{cn}(E_g)$	2127.6	98 $\nu_{cn}(E_g)$	2085.4	98 $\nu_{cn}(E_g)$	2121.2	99 $\nu_{cn}(E_g)$
ν_6	2044	2117.8	99 $\nu_{cn}(T_{1u})$	2117.3	100 $\nu_{cn}(T_{1u})$	2074.7	100 $\nu_{cn}(T_{1u})$	2115.4	100 $\nu_{cn}(T_{1u})$
ν_7	583	604.0	43 $\delta_l(T_{1u})$, 30 $\delta_a(T_{1u})$, 16 $\nu_{mc}(T_{1u})$	597.4	44 $\delta_l(T_{1u})$, 31 $\delta_a(T_{1u})$,14 $\nu_{mc}(T_{1u})$	606.2	55 $\delta_l(T_{1u})$, 31 $\delta_a(T_{1u})$, 12 $\nu_{mc}(T_{1u})$	538.7	51 $\delta_l(T_{1u})$, 37 $\delta_a(T_{1u})$
ν_{10}	510	514.5	57 $\delta_l(T_{2g})$, 31 $\delta_a(T_{2g})$	510.3	56 $\delta_l(T_{2g})$, 31 $\delta_a(T_{2g})$	526.8	69 $\delta_l(T_{2g})$, 30 $\delta_a(T_{2g})$	467.1	60 $\delta_l(T_{2g})$, 34 $\delta_a(T_{2g})$
ν_{12}		499.9	61 $\delta_l(T_{2u})$, 16 $\delta_a(T_{2u})$	497.2	61 $\delta_l(T_{2u})$, 16 $\delta_a(T_{2u})$	515.1	73 $\delta_l(T_{2u})$, 16 $\delta_a(T_{2u})$	466.5	62 $\delta_l(T_{2u})$, 21 $\delta_a(T_{2u})$
ν_8	416	417.8	81 $\nu_{mc}(T_{1u})$, 13 $\delta_l(T_{1u})$	407.0	83 $\nu_{mc}(T_{1u})$, 12 $\delta_l(T_{1u})$	411.9	84 $\nu_{mc}(T_{1u})$, 12 $\delta_l(T_{1u})$	300.3	91 $\nu_{mc}(T_{1u})$, 7 $\delta_l(T_{1u})$
ν_2	396	389.2	96 $\nu_{mc}(A_{1g})$	379.0	97 $\nu_{mc}(A_{1g})$	378.5	96 $\nu_{mc}(A_{1g})$	285.8	98 $\nu_{mc}(A_{1g})$
ν_4	376	388.2	96 $\nu_{mc}(E_g)$	377.8	96 $\nu_{mc}(E_g)$	377.3	96 $\nu_{mc}(E_g)$	280.0	98 $\nu_{mc}(E_g)$
ν_5		342.7	98 $\delta_l(T_{1g})$	341.8	100 $\delta_l(T_{1g})$	370.7	100 $\delta_l(T_{1g})$	330.2	100 $\delta_l(T_{1g})$
ν_9		125.2	79 $\delta_a(T_{1u})$, 52 $\delta_l(T_{1u})$	126.2	77 $\delta_a(T_{1u})$, 51 $\delta_l(T_{1u})$	145.8	70 $\delta_a(T_{1u})$, 34 $\delta_l(T_{1u})$	130.3	64 $\delta_a(T_{1u})$, 45 $\delta_l(T_{1u})$
ν_{11}	105	114.0	71 $\delta_a(T_{2g})$, 45 $\delta_l(T_{2g})$	114.4	70 $\delta_a(T_{2g})$, 45 $\delta_l(T_{2g})$	129.0	69 $\delta_a(T_{2g})$, 29 $\delta_l(T_{2g})$	115.4	66 $\delta_a(T_{2g})$, 40 $\delta_l(T_{2g})$
ν_{13}		77.1	99 $\delta_a(T_{2u})$, 55 $\delta_l(T_{2u})$	78.8	98 $\delta_a(T_{2u})$, 53 $\delta_l(T_{2u})$	95.1	86 $\delta_a(T_{2u})$, 29 $\delta_l(T_{2u})$	88.5	85 $\delta_a(T_{2u})$, 44 $\delta_l(T_{2u})$

[a]IR from reference 2 and Raman from reference 8.

single or double zeta basis set with/without polarization set. Calculated metal-ligand distances were ranging in 1.81 to 1.99 Å for low spin $^1A_{1g}$ state of ferrocyanide depending on the function method and basis set chosen. Pierloot *et al.*[24] took the Fe-C bond distance as 1.91 Å or 1.93 Å and the C≡N as 1.17 Å for the calculation of ligand field splitting energies. Therefore the Fe-C bond distance in the ferrocyanide complex ion is recognized to have about 1.90 Å.

Structural parameters of ferrocyanide optimized at different force fields are shown in Table 1. At Hartree-Fock level with the 6-31G** basis set, the Fe-C bond distance comes too long, and the C≡N very tight. The results from MP2/6-31G** or 6-31+G** basis set are shorter in Fe-C and too long in C≡N. At B3LYP level with the 6-31G(3df, 3pd) basis set, the bond Fe-C distance becomes much closer than at HF level, and that the C≡N is rather longer. With the 6-31+G** basis set, the bond distances of two become a little longer. With the 6-31G** basis set, the bond distances of them become a little closer. Isolated cyanide anion $C{\equiv}N^-$ shows a bond distance, 1.184 Å when optimized with the functional, B3LYP/6-31G**. This shows that an optimized C≡N distance in the ferrocyanide is almost the same as calculated in the isolated $C{\equiv}N^-$ anion. So, we retained to utilize the functional B3LYP/6-31G** for the ferrocyanide system. Because this calculated bond distance for Fe-C is rather extended over the usual metal-carbon distance in the metal hexacyano complex ions, we have chosen more realistic bond length, 1.90 or 1.91 Å for Fe-C. The calculated C≡N bond distance, 1.184 Å is rather longer than 1.17 Å taken in the previous works.

The electronic energies (ΔE_{elec}) and the summations (ΔG_T) of electronic and thermal free energy for geometries **A**, **B**, and **C** relative to the global minimum energy of fully optimized geometry **Opt** (2.009 Å for Fe-C, and 1.184 Å for C≡N) at B3LYP/6-31G** level are shown in Table 1. The geometry of A, B, and C adapted for calculation is off about 0.1 Å in Fe-C distances from optimized bond distance, therefore their free energies of formation are about 9 kcal/mol higher than optimized. Actually, our force constant calculation has been performed on the downhill side in the potential well, up by about 9 kcal/mol in the free energy from the minimum. This can cause a bit of off-symmetry in the force constant matrix, but it was small enough to be managed to handle. So, some of the force constants were averaged, but deviations were small enough less 1% and overall not significant.

Normal Mode Calculations. The symmetry force constants matrix for the geometry **Opt** is displayed in Table 4 in the matrix format of symmetry species coordinate. Table 4 shows only 13 diagonal and 10 off-diagonal elements in the matrix format, and other off-diagonal terms are ignored because they are near zero less than 0.004. There are three blocks of off-diagonal terms, *i.e.*, 3 positive elements of stretching-stretching interactions, 4 (one negative and three positive) elements of stretching-bending interactions, and 3 negative elements of angled bending-linear bending interactions. These elements in the matrix have exactly the same arrangement corresponding to the results of I. Nakagawa and T. Shimaouchi.[1] The notations by them for symmetry coordinates are added to the column and row in the bold faced **S** for the convenience. The symmetry force constants of geometry **A**, **B** and **C** are given in Table 5. Calculated frequencies are shown for geometry **A**, **B**, **C** and **Opt** in Table 6 along with potential energy distributions.

Three frequencies of C≡N stretching vibrations arise near 2100 cm^{-1} region, and highly localized as shown at the vibration numbers ν_1, ν_3, and ν_6. The vibration ν_5 with T_{1g} symmetry of the linear bending deformations is also highly localized because it is a sole symmetry in this system, but it is inactive in IR or Raman. Two of the Fe-C stretching modes, $\nu_{mc}(A_{1g})$ and $\nu_{mc}(E_g)$, are heavily localized at the

vibration ν_2 and ν_4, but the vibration ν_8 with T_{1u} symmetry is attributed mostly to $\nu_{mc}(T_{1u})$ and partly about 10% to $\delta_l(T_{1u})$ of linear bending deformations, as well. The region near 500 cm^{-1} to 600 cm^{-1} is contributed mainly with linear bending deformations and partly with angled bending deformations. Only the vibration ν_7 is containing a contribution from ν_{mc} (T_{1u}) about 10%. The low frequency region below 150 cm^{-1} is mainly from angled and linear bending deformations. The angled bending deformations contribute much more than the linear bending, however. In fact, except T_{1g} symmetry all the same symmetry species interacts more or less. Six terms out of total ten off-diagonal interaction constants are induced from interactions between T_{1u} symmetries, as can be seen in Table 4.

Extending of the Fe-C bond distance from 1.90 Å to 1.91 Å turns out to reduce the stretching frequencies of Fe-C, as expected. The stretching frequencies of C≡N bonds are unchanged basically considering that three modes of C≡N stretching have the same symmetry with Fe-C stretching and they can interact weakly 2 or 3% in potential energy distributions. But, it shows a mixed effect on two different deformations, *i.e.*, weakening linear bending deformations and strengthening angled bending deformations. But, these effects are not much noticeable. Lengthening the C≡N bond distance from 1.184 Å to 1.190 Å, the bands attributed to Fe-C stretching vibrations are unchanged almost. But, all deformations including angled and linear bending vibrations become stronger.

Viewing the PED values of geometry **A** and **B** on Table 6, the Fe-C bond distance does not give much impact on the potential energy distributions. However, extending the C≡N bond distance intensifies the separation of the linear bending and the angled bending deformations as seen in the cases of geometry **B** and **C**.

Table 4 and Table 5 display all effects on the force constants caused from geometrical displacements of the bond distance in Fe-C or C≡N. Every diagonal term depends on its bond distance. Among three blocks of off-diagonal terms, 3 positive terms of stretching-stretching interactions, and 3 negative terms of angled bending-linear bending interactions are dependent upon the bond distance. When the stretching-bending interaction terms, 4 (one negative and three positive) elements are less sensitive to the displacement of the bond distance. They all belong to T_{1u} symmetry, *i.e.*, (**S_6,S_8**), (**S_6,S_9**), (**S_7,S_8**) and (**S_7,S_9**) shown in Table 5.

Viewing PED of the geometry **Opt** shown in Table 6, the stretching modes of Fe-C and C≡N are highly localized compared to other geometries because the Fe-C bond distance is much longer than others. It turns out much less interaction force constants between two stretching modes and between angled and linear bending modes as can be seen in Table 4. Lengthening of the Fe-C bond distance has increased the angled bending force constants and decreased the linear bending force constants. These effects are represented in Table 6 as the frequency down-shifts for the vibration number ν_5, ν_7, ν_{10} and ν_{12} in great extents and as the frequency up-shifts for the vibration number ν_9, ν_{11} and ν_{13} in minor amounts.

Table 7. Observed and Calculated Vibrational Frequencies in cm^{-1} and Potential Energy Distributions through Non-linear least-square fitting Refinement for Geometry **B**

Vib. No.	Obs.[a]	Calc.	PED (greater than 5 %)		Vibration
ν_1	2098	2098.0	100 $\nu_{cn}(A_{1g})$		Raman
ν_3	2062	2062.0	100 $\nu_{cn}(E_g)$		Raman
ν_6	2044	2044.0	100 $\nu_{cn}(T_{1u})$		IR
ν_7	583	583.0	41 $\delta_l(T_{1u})$	32 $\delta_a(T_{1u})$ 20 $\nu_{mc}(T_{1u})$	IR
ν_{10}	510	510.0	53 $\delta_l(T_{2g})$	30 $\delta_a(T_{2g})$	Raman
ν_{12}		497.2	61 $\delta_l(T_{2u})$	16 $\delta_a(T_{2u})$	*inactive*
ν_8	416	416.0	76 $\nu_{mc}(T_{1u})$	15 $\delta_l(T_{1u})$	IR
ν_2	396	395.6	97 $\nu_{mc}(A_{1g})$		Raman
ν_4	376	375.7	97 $\nu_{mc}(E_g)$		Raman
ν_5		341.8	100 $\delta_l(T_{1g})$		*inactive*
ν_9		127.4	74 $\delta_a(T_{1u})$	49 $\delta_l(T_{1u})$	IR
ν_{11}	105	105.0	72 $\delta_a(T_{2g})$	50 $\delta_l(T_{2g})$	Raman
ν_{13}		78.8	98 $\delta_a(T_{2u})$	53 $\delta_l(T_{2u})$	*inactive*

[a]IR from reference 2 and Raman from reference 8.

Non-Linear Least Square Fitting. The least square fitting was carried out to minimize the square of differences of experimentally observed frequencies from calculated ones through refining the force constants. The minimization was done by the conjugate gradient method with a cube interpolation. The fitted frequencies and potential energy distributions for geometry **B** are given in Table 7. The PED values are very similar to those of Geometry B unfitted. But, the refined force constants in the symmetry coordinates shown in Table 5 are representing some singularities compared to the unfitted geometry **B**. The interaction terms between Fe-C stretching and C≡N stretching vibrations are increased nearly two times. Other interaction force constants are changed slightly.

Finding Internal Force Constants in the Modified Urey-Bradley Force Field. The modified Urey-Bradley type potential function employed by I. Nakagawa and T. Shimanouchi for $M(CN)_6^{x-}$ type octahedral metal cyanide species was represented as

$$2\,V = \sum K_1\,(\Delta r_i)^2 + \sum K_2\,(\Delta r_i')^2 + \sum H_1\,r_o^2(\Delta\alpha_{jk})^2 + \sum H_2 r_0 r_0'(\Delta\beta_i)^2 + \sum F\,(\Delta q_{jk})^2 + (\text{linear terms}) + 2\sum p_1\,(\Delta r_j)\,(\Delta r_l) + 2\sum p_2\,(\Delta r_i)\,(\Delta r_i')$$

where, r_i and r_i' are Fe-C and C≡N bond lengths with equilibrium distances, r_0 and r_0'; α_{jk} C-Fe-C angled bond angles; β_i Fe-C=N linear bond angles; q_{jk} distances between non-bonded carbon atoms. The constants K_1 and K_2 are Fe-C and C≡N bond stretching force constants, H_1 and H_2 C-Fe-C and Fe-C≡N bending force constants, F the repulsive force constant, and p_1 and p_2 the interaction force constants between two Fe-C bonds on the same diagonal and between adjacent Fe-C and C≡N bonds, respectively. The last two interaction terms are added to the ordinary Urey-Bradley potential functions.

To obtain the force constants employed in the modified

Table 8. Force Constants (mdyn/Å or equivalents) in the Internal Coordinates of the Modified Urey-Bradley Force Field for Geometry A, B, C and Opt, and the Values in Reference 1

Internal Coordinates in the Modified UB Force Field	Geometry **A** Fe-C: 1.90 Å C≡N: 1.184 Å	Geometry **B** Fe-C: 1.91 Å C≡N: 1.184 Å	Geometry **C** Fe-C: 1.91 Å C≡N: 1.190 Å	Geometry **Opt** Fe-C: 2.009 Å C≡N: 1.184 Å	Force Constants employed in the Modified UB Force Field
Δr(Fe-C)	1.9983	1.8857	1.8810	1.004	K_1 = 2.4828[b]
Δr(C≡N)	17.0780	17.0807	16.4005	17.1164	K_2 = 15.1[b]
Δα(C-Fe-C)[a]	0.1941 (T_{1u})	0.1953 (T_{1u})	0.2125 (T_{1u})	0.2653 (T_{1u})	H_1 = 0.039[c]
	0.1256 (T_{2g})	0.1250 (T_{2g})	0.1329 (T_{2g})	0.1840 (T_{2g})	
	0.1228 (T_{2u})	0.1271 (T_{2u})	0.1437 (T_{2u})	0.2189 (T_{2u})	
Δβ(Fe-C≡N)	0.1896	0.1871	0.2337	0.1731	H_2 = 0.172[b]
Δq(C ⋯ C)	-0.0649	-0.0650	-0.0657	-0.0638	F = 0.111[c]
Δr(Fe-C, Fe-C)	-0.2015	-0.2005	-0.2033	-0.2579	p_1 = -0.172[c]
Δr(Fe-C, C≡N)	0.3632	0.3520	0.3503	0.2469	p_2 = 0.4[c]

[a]Because the internal coordinates of the angled bending deformations are not linearly independent, values converted to hold the same unit in the symmetry coordinate are shown instead. [b]adjusted values for the calculated frequencies to fit to the observed frequencies. [c]fixed to predetermined values.

Urey-Bradley type potential function, the input file for generating the symmetry coordinates in Table 3 was partly modified. The stretching coordinates of Fe-C and C≡N bonds and the linear bending coordinates of Fe-C≡N bond are set to their internal coordinates (**R**) because the number of symmetry coordinates is the same as that of internal coordinate, and they are independent. However, the symmetry coordinates for the angled bending coordinates were used as displayed in Table 3 because the internal coordinates of the angled bending deformations are not linearly independent. Therefore, the force constants, H_1, of the angled bending deformations cannot be evaluated independently in the internal coordinates due to the redundancy. Applying this modified input coordinate file, the values of K_1, K_2, and H_2 can be obtained on the diagonal terms of the force constant matrix directly. These are listed in Table 8.

Values for the interaction terms can be calculated using equations of F_{ij} elements shown in Table 5. The F value was obtained using the (**S**$_7$,**S**$_9$) interaction term in the symmetry coordinates which was defined to $0.9r_oF$. The (**S**$_7$,**S**$_9$) term is generated from an interaction between the Fe-C stretching vibration and the C-Fe-C angled bending deformation with T_{1u} symmetries. The Fe-C stretching vibration with T_{1u} symmetry is that two carbon atoms on a certain 4-fold rotational axis move forward and the centered metal atom backward on the axis, and others are fixed. The C-Fe-C angled bending deformation with T_{1u} symmetry is that four carbon atoms perpendicular to a certain 4-fold rotational axis move backward parallel to that axis, the centered metal atom forward on that axis. Combining both of symmetry coordinates results in a vibrational motion of only six carbon atoms holding a centered metal atom and six nitrogen atoms at fixed positions. Two carbon atoms on the same diagonal move forward and other four carbon atoms backward, or vice versa. This motion could be regarded as an interaction of non-bonded carbon atoms.

The interaction constants, p_2 between adjacent Fe-C and C≡N stretching are present in terms of (**S**$_1$,**S**$_2$), (**S**$_3$,**S**$_4$) and (**S**$_6$,**S**$_7$) interactions crossed in the same symmetry block in Table 4. As these values are quite similar to each other, so averaged to give p_2. The effect of this p_2 interaction constant is marginal to the Fe-C or C≡N stretching vibrations. Coupling of these two modes is not significant, usually negligible even though its value is near 0.35.

The interaction constants, p_1 are embedded in (**S**$_2$,**S**$_2$), (**S**$_4$,**S**$_4$), and (**S**$_7$,**S**$_7$) as indicated in Table 5. It was defined as an interaction between two Fe-C stretching vibrations on a 4-fold rotational axis in the octahedral geometry. The symmetry coordinate of $\nu_{mc}(A_{1g})$ in Table 3 was represented as +R1+R2+R3+R4+R5+R6, and $\nu_{mc}(E_g)$ as +2R1-R2-R3+2R4-R5-R6. Mixing of two coordinates with different symmetries could end to R1+R4. It is an extending motion of only two Fe-C bonds, and any other atoms remaining unchanged in position. The values of p_1 were obtained for two symmetry species, *i.e.*, A_{1g} and E_g, respectively. Then, the p_1 of E_g symmetry was subtracted from the p_1 of A_{1g} symmetry to get as the true value of p_1. This value was signed negative because this motion is unfavorable to symmetry.

The force constants, H_1 of C-Fe-C angled bending deformations are also embedded in (**S**$_9$,**S**$_9$) of T_{1u}, (**S**$_{11}$,**S**$_{11}$) of T_{2g} and (**S**$_{13}$,**S**$_{13}$) of T_{2u} symmetry in the symmetry coordinates. For three symmetries, values of H_1 were calculated using F previously obtained, and listed in Table 8. Because the internal coordinates of angled bending deformations have 3 redundant coordinates, it is not possible to get the force constant in the internal coordinates. Therefore the H_1 values for three symmetry coordinates were obtained, instead. The force constants of angled bending deformations were obtained about 3 to 5 times higher dependent on the symmetry than the value by I. Nakagawa and T. Shimanouchi. In other study[6] of ferricyanide, $[Fe(CN)_6]^{3-}$, by I. Nakagawa and T. Shimanouchi, H_2 value was reported 0.8 which is very close to our value of angled bending deformation with T_{1g} symmetry. (Table 4 The interaction constant F for non-bonded carbon atoms is about half comparing to their value. The values of the interaction constants, p_1 and p_2 obtained in this work are similar to those.

Table 9. Valence Force Constants (mdyn/Å or equivalents) in the General Quadratic Valence Force Field for Geometry A, B, C and Opt and Refined Valence Force Constants of Geometry B

Symmetry *F* Matrix Elements[a]	Geometry A	Geometry B	Geometry C	Geometry Opt	Refined Constants of Geometry **B**
$F_{Fe\text{-}C}$	1.9982	1.8858	1.8810	1.0040	1.952
$F_{C\equiv N}$	17.0780	17.0813	16.4006	17.1091	16.230
$F^{c}_{C\equiv N,C'\equiv N'}$	0.0979	0.0963	0.0950	0.0827	0.095
$F^{t}_{C=N,C'\equiv N'}$	0.0835	0.0813	0.0816	0.0592	0.230
$F^{c}_{Fe\text{-}C,Fe\text{-}C'}$	0.0021	0.0023	0.0023	0.0079	0.040
$F^{t}_{Fe\text{-}C,Fe\text{-}C'}$	0.3642	0.3487	0.3497	0.2244	0.312
$F_{Fe\text{-}C,C\equiv N}$	0.3638	0.3509	0.3494	0.2316	0.602
$F^{c}_{Fe\text{-}C,C'\equiv N'}$	-0.0022	-0.0005	-0.0007	0.0139	0.011
$F^{t}_{Fe\text{-}C,C'\equiv N'}$	0.0026	0.0044	0.0042	0.0182	0.079
$F_{\alpha} - F_{\alpha\alpha''}$	0.7010	0.7185	0.7816	0.8356	0.715
$F_{\alpha\alpha'} - F_{\alpha\alpha'''}$	0.0643	0.0622	0.0627	0.0468	0.060
$F_{\alpha} - F_{\alpha\alpha''''}$	0.6416	0.6523	0.6991	0.7183	0.634
F_{β}	0.4265	0.4232	0.5311	0.3887	0.407
$F_{\beta\beta'}$	0.0369	0.0359	0.0513	0.0286	0.038
$F_{\beta\beta''}$	0.0280	0.0272	0.0427	0.0203	0.018
$F_{\beta\beta'''}$	0.0089	0.0087	0.0088	0.0069	0.002
$F_{\alpha\beta'}$	-0.0802	-0.0772	-0.0294	-0.0487	-0.081
$F_{\alpha\beta''}$	-0.0438	-0.0430	-0.0273	-0.0346	-0.029
$F_{\alpha\beta'''}$	0.0045	0.0046	0.0048	0.0057	0.010
$F_{C\equiv N,\beta'}$	0.0135	0.0131	0.0134	0.0116	0.013
$F_{C\equiv N,\alpha'} - F_{C\equiv N,\alpha''}$	0.0850	0.0822	0.0819	0.0584	0.082
$F_{Fe\text{-}C,\beta'}$	0.0155	0.0154	0.0152	0.0148	0.013
$F_{Fe\text{-}C,\alpha'} - F_{Fe\text{-}C,\alpha''}$	-0.0555	-0.0559	-0.0565	-0.0577	-0.059

[a]from Reference 12.

Finding Valence Force Constants in the General Quadratic Valence Force Field. The force constants in the internal coordinates are more informative than symmetry force constants because of their transferability. The valence force constants in the general quadratic valence force field were obtained and given in Table 9 as done for the same symmetry species,[12] $Cr(CO)_6$. Considering the geometry **A**, **B**, **C** and **Opt** in Table 9, one can notice that the Fe-C bond distance gives much milder impacts on the force constants of all, but the C≡N bond distance does stronger on the selected force constants.

The interaction constants between stretching and stretching are not much subject to change upon geometrical displacement as can be seen in Table 9. The *cis* interactions, $F^{c}_{C\equiv N,C'\equiv N'}$, $F^{c}_{Fe\text{-}C,Fe\text{-}C'}$, and $F^{c}_{Fe\text{-}C,C'\equiv N'}$, are small or essentially zero. In the study[12] of $Cr(CO)_6$, $F^{c}_{C\equiv O,C'\equiv O'}$ was obtained about 0.2 mdyn/Å which is nearly twice of ferrocyanide. Other two *cis* interactions were also closely negligible in $Cr(CO)_6$. Among the *trans* interactions, the constant $F^{t}_{Fe\text{-}C,Fe\text{-}C'}$ has a significant value of about 0.35 mdyn/Å, but other two *trans* constants $F^{t}_{C=N,C'=N'}$ and $F^{t}_{Fe\text{-}C,C'=N'}$, are relatively small. The $F_{Fe\text{-}C,C=N}$ is about 0.35 mdyn/Å for three geometries, but through the least-squares refinement to experimental frequencies it results in 0.602 mdyn/Å as can be seen in the rightmost column in Table 9, which is not far from 0.68 mdyn/Å of $Cr(CO)_6$.

When weakening the C≡N bond order from geometry B to C, the force constants of angled bending (F_{α}) and linear bending (F_{β}) deformations are getting significantly increased. Therefore the angled bending or linear bending deformations are strongly dependent on the C≡N bond distance as can be conformed from calculated frequencies in Table 6. The interaction force constants ($F_{\alpha\beta'}$ and $F_{\alpha\beta''}$) between angled bending and linear bending deformations are small enough, and they are also dependent on the distance of C≡N as much. The interaction force constants between stretch (Fe-C or C≡N) and bending (angled or linear) are all small, and very insensitive to the geometrical displacement. The stretch-angled bending interactions ($F_{C\equiv N,\alpha'}$-$F_{C\equiv N,\alpha''}$ and $F_{Fe\text{-}C,\alpha'}$-$F_{Fe\text{-}C,\alpha''}$) are larger than the stretch-linear bending interactions ($F_{C\equiv N,\beta'}$ and $F_{Fe\text{-}C,\beta'}$). This is in the same manner with the case[12] of $Cr(CO)_6$.

Refined force constants of geometry **B** through least-square fitting procedure using experimentally observed frequencies shown in Table 7 are similar to valence force constants of geometry B except several force constants. The constants $F_{Fe\text{-}C}$ and $F_{C\equiv N}$ are calculated to 1.952 and 16.230 mdyn/Å, respectively. Reported values[10] previously for ferrocyanide ion were 1.99 and 15.52, respectively, which were obtained using 10-parameter potential function in the valence force field. The value of $F_{C\equiv N}$ is a little lower than usual, partly because we have chosen a bit longer bond distance for C≡N, 1.184 Å. The linear bending force constants (F_{β}, $F_{\beta\beta'}$, $F_{\beta\beta''}$, and $F_{\beta\beta'''}$) and the interaction constants ($F^{t}_{C\equiv N,C'\equiv N'}$ and $F^{c}_{C\equiv N,C'\equiv N'}$) are comparable to the values reported.[10] The interaction constants, $F^{t}_{C\equiv N,C'\equiv N'}$ and $F_{Fe\text{-}C,C\equiv N}$ for ferricyanide ion,[11(b)] $[Fe(CN)_6]^{3-}$, were evaluated to 0.2 and 0.2 mdyn/Å, respectively. In this study of ferrocyanide, these interaction constants come out to 0.230 and 0.602 mdyn/Å, respectively.

Conclusions

Vibrational properties of ferrocyanide complex ion, $[Fe(CN)_6]^{4-}$, have been studied based on the force constants obtained from the density functional calculations at B3LYP/6-31G** level. This study was conducted by means of the normal mode analysis through Wilson's *GF* matrix method using new bond angle and linear angle internal coordinates recently developed. Three different geometries with moderate bond distances have been adapted to obtain the effects of geometrical displacements. The density functional calculations at this level reproduced vibrational frequencies of ferrocyanide adequately. The refined force constants in the symmetry coordinate as well in the internal coordinate were also attempted to retrieve using experimentally observed frequencies by non-linear least-square fitting method.

The internal force constants were evaluated in the general quadratic valence force field and the modified Urey-Bradley force field. In the modified Urey-Bradley force field, the

angled bending force constants previously reported were about five times underestimated, but the interaction constant for non-bonded carbon atoms is about two times overestimated. The values of the interaction constants, p_1 and p_2 obtained from density functional force field are similar to those employed previously. In the valence force field, the stretch-stretch interaction and stretch-bending interaction constants are not sensitive to the geometrical displacement in the valence force field. Most of interaction force constants of ferrocyanide are comparable to those of $Cr(CO)_6$ well studied, and could be regarded to be transferable appropriately to other hexacyano transition metal complexes.

Acknowledgment. This paper is dedicated to Prof. Kyung-Hoon Jung on the occasion of his 65th anniversary.

References

1. Nakagawa, I.; Shimanouchi, T. *Spectrochim. Acta* **1962**, *18*, 101.
2. Jones, L. H. *Inorg. Chem.* **1963**, *2*, 777.
3. Bloor, D. *J. Chem. Phys.* **1964**, *41*, 2573.
4. Nakagawa, I.; Shimanouchi, T. *Spectrochim. Acta* **1966**, *22*, 1707.
5. Nakagawa, I.; Shimanouchi, T.; Yamasaki, K. *Inorg. Chem.* **1968**, *7*, 1332.
6. Nakagawa, I.; Shimanouchi, T. *Spectrochim. Acta* **1970**, *26A*, 131.
7. Swanson, B. I.; Jones, L. H. *J. Chem. Phys.* **1970**, *53*, 3761.
8. Griffith, W. P.; Turner, G. T. *J. Chem. Soc. (A)* **1970**, 858.
9. (a) Swanson, B. I.; Jones, L. H. *J. Chem. Phys.* **1971**, *55*, 4174. (b) Jones, L. H.; Swanson, B. I.; Kubas, G. J. *J. Chem. Phys.* **1971**, *55*, 4174.
10. Hipps, K. W.; Williams, S. D.; Mazur, U. *Inorg. Chem.* **1984**, *23*, 3500.
11. (a) Swanson, B. I.; Jones, L. H. *Inorg. Chem.* **1974**, *13*, 313. (b) Jones, L. H.; Swanson, B. I. *Acc. Chem. Res.* **1976**, *9*, 128.
12. Jones, L. H.; McDowell, R. S.; GoldBlatt, M. *Inorg. Chem.* **1969**, *8*, 2349.
13. (a) Fan, L.; Ziegler, T. *J. Phys. Chem.* **1992**, *96*, 6937. (b) Sosa, C.; Andzelm, J.; Elkin, B. C.; Wimmer, E.; Dobbs, K. D.; Dixon, D. A. *J. Phys. Chem.* **1992**, *96*, 6630.
14. (a) Bérces, A.; Ziegler, T.; Fan, L. *J. Phys. Chem.* **1994**, *98*, 1584. (b) Bérces, A.; Ziegler, T. *J. Phys. Chem.* **1995**, *99*, 11417. (c) Ziegler, T. In *Density Functional Methods in Chemistry and Materials Science*; Springborg, M., Ed.; John Wiley and Sons: U.K., 1997; p 69.
15. Lee, C.; Yang, W.; Parr, R. G. *Phys. Rev. B* **1988**, *37*, 785.
16. Lee, S.-H.; Krimm, S. *Biopolymer* **1998**, *48*, 283.
17. (a) Durig, J. R.; Yu, Z.; Guirgis, G. A. *J. Phys. Chem. A* **2000**, *104*, 741. (b) Park, S.-K.; Lee, N.-S.; Lee, S.-H. *Bull. Korean Chem. Soc.* **2000**, *21*, 959.
18. Lee, S.-H.; Palmo, K.; Krimm, S. *J. Comput. Chem.* **1999**, *20*, 1067.
19. Rauhut, G.; Pulay, P. *J. Phys. Chem.* **1995**, *99*, 3093.
20. Frisch, M. J.; Trucks, G. W.; Schlegel, H. B.; Scuseria, G. E.; Robb, M. A.; Cheeseman, J. R.; Zakrzewski, V. G.; Montgomery, J. A., Jr.; Stratmann, R. E.; Burant, J. C.; Dapprich, S.; Millam, J. M.; Daniels, A. D.; Kudin, K. N.; Strain, M. C.; Farkas, O.; Tomasi, J.; Barone, V.; Cossi, M.; Cammi, R.; Mennucci, B.; Pomelli, C.; Adamo, C.; Clifford, S.; Ochterski, J.; Petersson, G. A.; Ayala, P. Y.; Cui, Q.; Morokuma, K.; Malick, D. K.; Rabuck, A. D.; Raghavachari, K.; Foresman, J. B.; Cioslowski, J.; Ortiz, J. V.; Baboul, A. G.; Stefanov, B. B.; Liu, G.; Liashenko, A.; Piskorz, P.; Komaromi, I.; Gomperts, R.; Martin, R. L.; Fox, D. J.; Keith, T.; Al-Laham, M. A.; Peng, C. Y.; Nanayakkara, A.; Gonzalez, C.; Challacombe, M.; Gill, P. M. W.; Johnson, B.; Chen, W.; Wong, M. W.; Andres, J. L.; Gonzalez, C.; Head-Gordon, M.; Replogle, E. S.; Pople, J. A. *Gaussian 98*, Revision A.7; Gaussian, Inc.: Pittsburgh, PA, 1998.
21. Sano, M.; Kashiwagi, H.; Yamatera, H. *Inorg. Chem.* **1982**, *21*, 3837.
22. Mandix, K.; Hohanson, H. *J. Phys. Chem.* **1992**, *96*, 7261.
23. Bolvin, H. *J. Phys. Chem. A* **1998**, *102*, 7525.
24. Pierloot, K.; Praet, E. V.; Vanquickenborne, L. G.; Roos, B. O. *J. Phys. Chem.* **1993**, *97*, 12220.